Volume Loading—A New Principle for Small Antennas

Douglas B. Miron
Siouxland Scientific Computing
221 17th Avenue
Brookings, SD 57006

Abstract

Volume loading means placing conductively enclosed volumes at the ends of the arms of a short linear antenna to increase and control the capacitance of the structure. This technique allows tuning the antenna to make it series-resonant at a design frequency for which it is electrically small. This paper describes the discovery and development of the concept, gives some computed examples to illustrate the relation between shape and performance, and describes some experimental work, including a 900 MHz cordless phone demonstration design.

1. Introduction

Short monopoles and dipoles have two basic problems, low radiation resistance, and highly reactive input impedance. "Short" in this paper means less than $\lambda_0/8$ (one-eighth operating or design wavelength) for the equivalent dipole. These characteristics produce inefficiency in either the antenna or its connecting impedance-matching network, or both[1,2,3]. The low radiation resistance is due in part to the requirement that the conduction current has to go to zero at the open arm ends, and in part to the short length of the radiating current path. Traditional remedies use the addition of a circuit or structure along the antenna arms to give the conduction current some place to go after it gets to the arm end, and, in some cases, to tune the input impedance[4,5,6]. These loading structures are either series coils, capacitive plates or wire assemblies, or both. Capacitive end elements allow the current to spread out over their surface, going to zero at the edge of the assembly, so that its amplitude along the antenna arms stays nearly constant. This helps increase the radiation resistance but still leaves the input impedance quite reactive. Series coils improve the impedance-matching but decrease the efficiency of the antenna.

This paper describes a new class of shapes for electrically-small antennas. It is shown that end bodies which allow the conduction current to leave the arm end and flow around a volume back to the axis line of the antenna can be used to produce series resonance at the operating wavelength in a space which is still electrically small. We call this "volume loading". The result is a dipole or monopole antenna with as high a radiation resistance as the space allows and which minimizes the associated matching network loss.

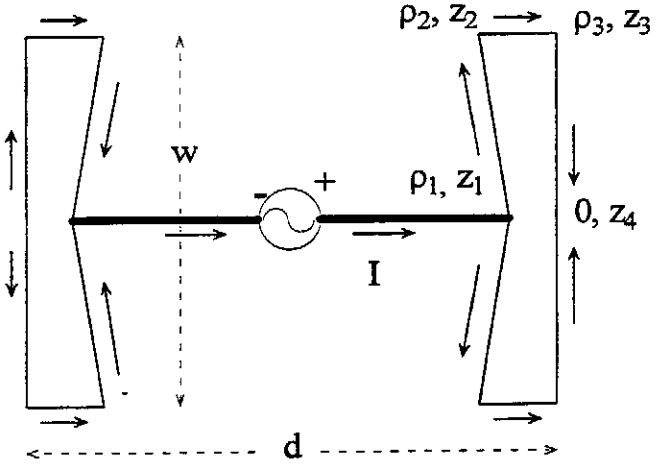

Figure 1. An illustration of volume loading applied to a short dipole. The antenna occupies a space defined by its overall length 'd' and its overall width 'w'. The corners of its straight-line-segmented half-profile are marked in cylindrical coordinates, ρ and z. The end bodies are the loading volumes, from z_1 through z_4.

A schematic drawing of a volume-loaded short dipole is shown in Figure 1. The Figure can be thought of either as a wire construction, or as a profile for a figure of revolution structure. These are, in fact, two extreme possibilities for implementation, though other body shapes are possible and will function in a similar manner. The nature of the antenna behavior is the same in both cases. In transmitter mode, current is driven along the arms of the dipole, as indicated by the arrows. When it reaches the arm end, it spreads out and travels in a symmetrical fashion around the space enclosed by the end body. If the dimension "w" of the body is comparable to the overall length, "d", the detail dimensions can be chosen so that the terminal impedance of the antenna will exhibit a series resonance at a frequency such that "d" is $\lambda_0/8$ or smaller. The ratio $\lambda_{0/d}$ has been found to depend on body shape and arm diameter. The shape of the end body can be made to produce enough capacitance to resonate with the arm inductance. This is illustrated in later sections.

The following section presents the background of the discovery of the volume-loading principle. some experimental results which support the main numerically-predicted properties are described in section 3, and section 4 numerically explores the dependence of performance

parameters on shape. Section 5 describes the development of a 900 MHz cordless phone antenna set and its operation. The last section gives the concluding discussion.

2. Background

Using a code [7], based on [8], we first discovered this class of shapes by numerical experiment. The original purpose of the code was to find a minimum-Q shape for very small dipoles. In the course of that study, a fairly low-frequency resonance was observed for some cases. A few years later, the dependence of this resonance on shape was numerically explored. In 1994, we decided to develop a wire approximation to the surface shape of the math model. We chose to build a simple design in the HF band. A square cross-section end body was used to approximate a 15 MHz design for which $d/\lambda_0=0.1$. This first attempt was quite successful, exhibiting a series resonance at about 16 MHz, so a second prototype was designed to approximate a 12 MHz, $d/\lambda_0=0.08$ design. The second prototype was built using an octagonal cross-section end body frame. A photo of the second prototype is shown in Figure 2. It too was quite successful and the measurements made on this model are described in the next section.

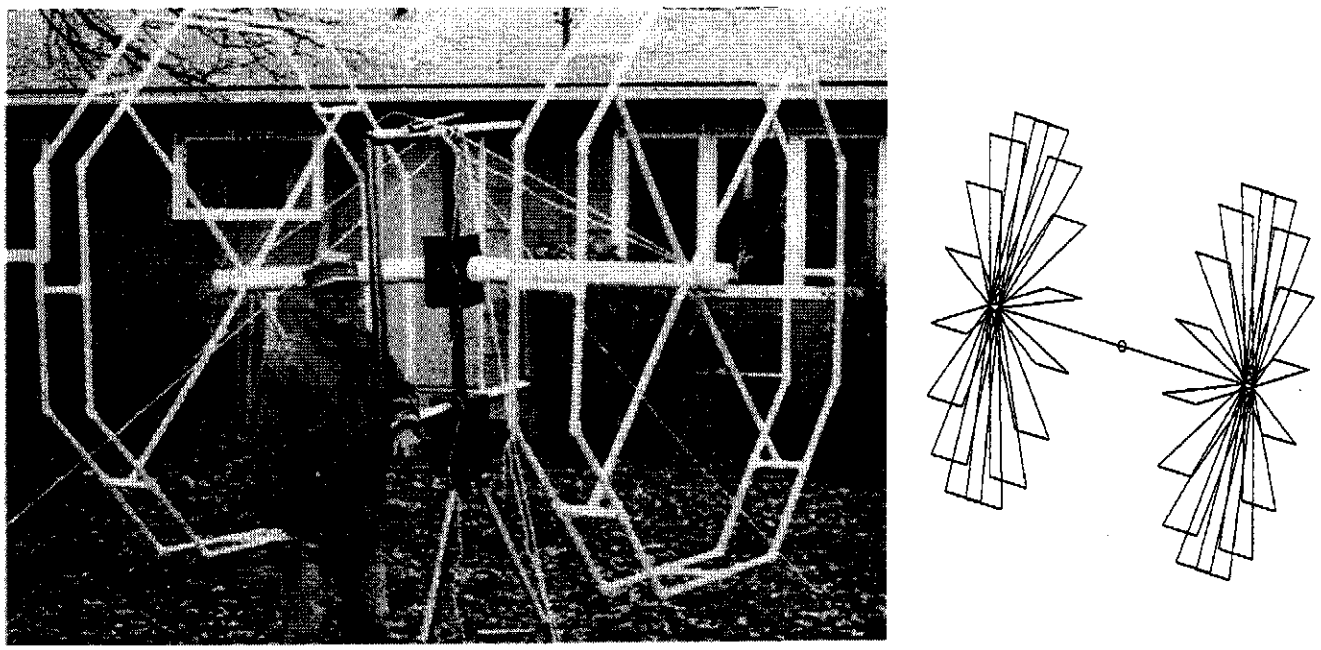

(a) (b)

Figure 2. (a) Photo of the second HF-band prototype. The wires are almost invisible. The structure was hung on the center post of a square stainless-steel loop which was made for other experiments. The white PVC tubing is used to make frames for the wires forming the end bodies. The next-most-visible objects are the white guy lines used to stabilize the structure. The dipole arms were each made of a single #14 copper wire passing through the 3" pipe to a distribution assembly near its end on the inside. (b) A drawing of the wires from EZNEC-M.

3. HF Prototype Construction and Tests

Both prototypes were built on PVC plastic pipe frames since the wire would not be self-supporting. Number 14 copper wire was used for the arms, and brought out and around the frame and terminated by a wrap around a 1/2 in. bolt in line with the arm. The profile of the figure of revolution is described by radial and axial distance values at each corner in the half-length profile, collected in vectors. For the second prototype these are, in meters,

ρ_d =[0.000814, 1, 1, 0],
z_d = [0.94, 0.74, 1, 1].

ρ_1, the first element of ρ_d, is the radius of the #14 wire, and z_1, the first element of z_d, is the z-axis position of the arm end, the feedpoint being taken as z=0. See Figure 1.

Measurements were made as the wiring was done. That is, the impedance of the terminal assembly was measured without any wire attached. The equivalent circuit here is a small series inductance and shunt capacitance. Then the framework was put up, and the impedance for a single wire going just straight out from each terminal was measured, then a half-loop put on each end, measured, then the loop completed and impedance-measured, and so on, until 8 full loops were in place at each end. This process allowed

observation of the development of the series resonance, which first appeared below 36 MHz with one complete loop at each end and then moved down in frequency as more loops were added. Table 1 shows the resonant frequency as a function of the number of loops at each end.

Table 1. Series-resonance frequency as a function of the number of end-body wire loops, N.

N	1	2	4	8
f, MHz	19.9	16.5	14	12.5

The instrument used for the measurements was an Autek RF-1 RF Analyst. It measures impedance magnitude and SWR over limited ranges, so the sign of the reactance has to be inferred. See the Appendix. Figure 3 gives the reactance of the antenna after the effects of the terminal equivalent circuit are removed, and the calculated reactance for the solid figure of rotation. The resistance at the 12.5 MHz resonance was about 8 Ω.

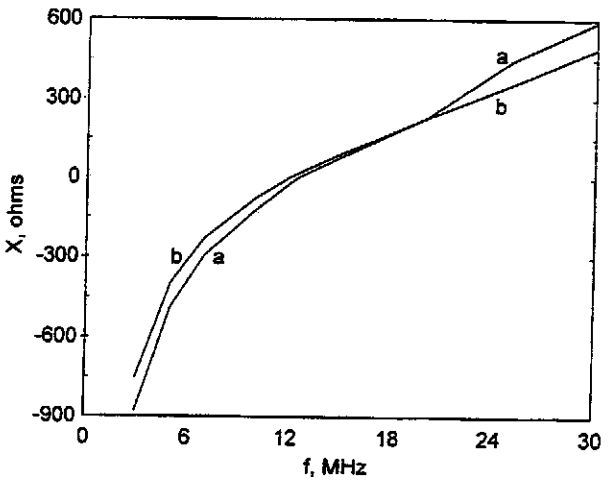

Figure 3. Reactance versus frequency, (a) inferred from measurements on the wire antenna, and (b) calculated for the figure of revolution antenna.

These measurements indicate that the code results are probably accurate, and that the measured resonant frequency will approach the code value as the number of end-body loops increases. It should be noted that the calculated values are for the body-of-revolution in free space, whereas the measurements were made about 1.8 m above ground.

4. Performance as a Function of Shape

In general, antenna performance is described in terms of radiation patterns, terminal impedance, and efficiency. For the antennas considered here, the computed radiation pattern is that of the classic short dipole, regardless of end body. Therefore only terminal properties and efficiency are of interest with respect to shape.

An electrically-small dipole with thin end plates is essentially a capacitor in which the conduction current has a path along the arm and is then allowed to spread out over the insides of the plates, going to zero current at the plate edge. It is superior to an unloaded small dipole because the amplitude of the radiating current stays near its feedpoint value, since it doesn't have to go to zero at the arm end. Also, the plate-loaded antenna has a lower reactance than the straight wire by itself. In the volume-loaded dipole, the current doesn't stop at the edge of the inner body face, but decreases slowly on the inner face, drops sharply between the two outside edges, finally tapering to zero current at the center of the face away from the arm end. The structure becomes a tuned system, with inductance from the wire arms in series with capacitance due to charge at the outer edges of the end bodies. This is illustrated in the calculated performance values given in the following tables and figures. As wavelength is increased, it is necessary to increase either L or C to achieve resonance in a fixed volume. The inductance is increased by making the arm thinner or longer (decreasing ρ_1 or increasing z_1), and the capacitance is increased by bringing the outer edges of the end volumes closer together (decreasing z_2).

In the two following tables, "w" and "d" are fixed at 2 m, so that the half-length of the dipole is 1 m. Equivalently, ρ_2, ρ_3, and z_4 are held at 1 m. These are examples of doing the best we can in a given three-dimensional space. Q_L is the inverse of the fractional bandwidth when driven from a source whose impedance is the resonant radiation resistance Rrad of the antenna. Rrad, the efficiency η, Q_L and λ_0, the resonant wavelength, are the performance parameters tabulated. The equivalent series-circuit element values are also listed.

The code used to calculate these values is a modified version of [7] in which the segments, instead of being constant length along the whole profile, are adjusted to have a length along each straight-line section of the profile so that each corner is also the end of a segment. This procedure gives more stable results than the original. The code still solves the EFIE as if the structure is a perfect conductor and then calculates loss resistance as if the loss were small enough not to affect the currents. For this reason, no cases for which the loss resistance is greater than 10 % of the radiation resistance (η<90 %) are given.

Table 4 illustrates the effect of relaxing the restriction on "w". The basic effect is to improve bandwidth, since the volume occupied is larger than the previous cases.

Table 2. λ_0=20. ρ_d=[ρ_1, 1, 1, 0], z_d=[z_1, z_2, 1, 1], in meters.

ρ_1 m	z_1 m	z_2 m	R_{rad} Ω	η %	Q_L	L, μH	C, pF
0.01	1	0.767	6.37	99.5	26.9	1.82	61.8
0.005	1	0.96	7.62	99.1	26.8	2.17	51.9
0.002	0.877	1	7.61	98.2	28.2	2.28	49.4

Table 3. λ_0=25, ρ_d =[ρ_1, 1, 1, 0], z_d=[z_1, z_2, 1, 1], in meters .

ρ_1 m	z_1 m	z_2 m	R_{rad} Ω	η %	Q_L	L, μH	C, pF
0.005	1	0.335	2.12	97.2	66.4	1.87	94
0.002	1	0.548	3.09	95.5	57.2	2.34	75.1
0.001	1	0.701	3.77	92.8	53.8	2.69	65.4

Table 4. Some examples with larger "w".

λ_0=20, ρ_d =[ρ_1, 1.5, 1.5, 0], z_d=[z_1, z_2, 1, 1], in meters.

ρ_1 m	z_1 m	z_2 m	R_{rad} Ω	η %	Q_L	L, μH	C, pF
0.01	0.513	1	6.69	99.7	16.8	1.19	94.4

λ_0=30, ρ_d =[ρ_1, 1.5, 1.5, 0], z_d=[z_1, z_2, 1, 1], in meters.

ρ_1 m	z_1 m	z_2 m	R_{rad} Ω	η %	Q_L	L, μH	C, pF
0.002	1	0.836	3.02	95.8	53.3	2.56	98.9
0.001	1	0.969	3.42	92.8	52.9	2.88	88.1

λ_0=30, ρ_d =[ρ_1, 2, 2, 0], z_d=[z_1, z_2, 1, 1], in meters.

ρ_1 m	z_1 m	z_2 m	R_{rad} Ω	η %	Q_L	L, μH	C, pF
0.005	0.808	1	3.31	98.7	36.7	1.94	131
0.002	0.649	1	3.14	97.3	37.2	1.86	137

The shapes of the volumes listed in Table 2-4 fall into two categories, convex ($z_1<z_2$) or concave ($z_1>z_2$). It follows that in some cases it is possible to find an arm radius for which the inside face of the end body is flat. Not only is this true, but the values of arm radius and plate thickness which give the desired resonant wavelength in the specified volume are not unique. Indeed, in the range $8<\lambda_0/d<10$ and w=d it is even possible to find a wire arm and wire radial assembly which is series resonant without incurring much loss. All the entries in Table 3, λ_0/d=12.5, are concave because decreasing the arm wire size to increase the inductance, allowing less capacitance and concavity, would have increased the loss above the 10 % point. Table 3 also shows clearly the negative effect of increasing concavity on the radiation resistance. This is due to the negative z component of the current on the concave face which produces a field opposite to that of the arm. Table 4 shows that increasing convexity also leads to reduced radiation resistance.

We have stated above, in effect, that the design process for a volume-loaded antenna is to balance the arm inductance and the end-body capacitance. The end-body capacitance is, to a first approximation, that of ring charges located on the volumes' outer edges. This is shown in the following two Figures. Figure 4 plots the computed current and charge distribution for a concave volume, and Figure 5 plots current and charge for a convex volume.

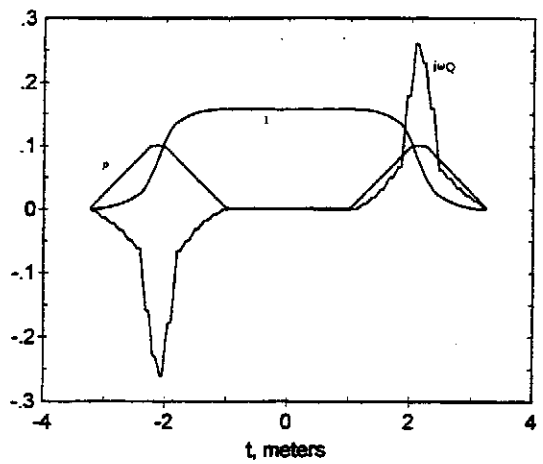

Figure 4. Current and charge for the dipole of Table 2, arm radius of .01. "I" is the total current at a given tangential point "t", "Q" is the corresponding charge density given by jωQ=-dI/dt. "ρ" is the profile radius, which is scaled and plotted to make it clear that the maximum charge density occurs at the plate's outer edges.

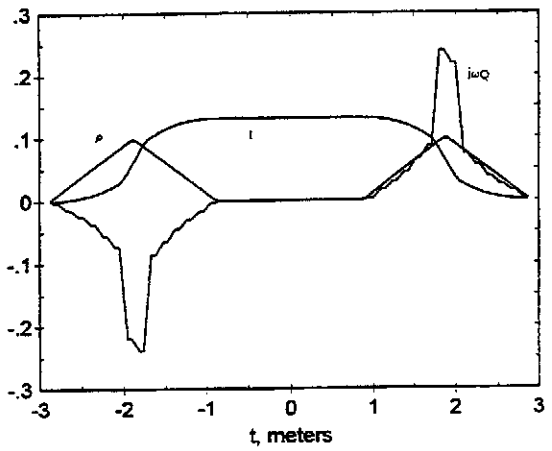

Figure 5. Current and charge for the antenna of Table 2 with arm radius=0.002 m. Label definitions are the same as for Figure 4.

At resonance, the current is real all along the profile, so the quantities plotted are the real parts, the imaginary parts being very small. The profile radius is also plotted in order to help clarify the position on the profiles. The independent coordinate is the tangential position. Since the arm length and each face radius are about 1 m, the half-dipole profile length is about 3 m, either side of the center feed point. The source is a 1 V delta gap model. It can be seen that the charge density is much higher at the maximum radius than elsewhere on the structure. Adjusting the z distance between these two ring charges is the chief means of adjusting the effective capacitance. The advantage that volume-loading has over simple plate-loading is that the charge is concentrated at the outer edge, giving a larger capacitance in a given space.

5. A 900 MHz Cordless Phone Application

In early 1996, it was decided to design and build a cordless phone demonstration set to illustrate some practical possibilities. We purchased a cordless phone, model ET-900, at a local Radio Shack store and ordered the service manual for it as well. The phone is a set consisting of a base unit and a battery-powered hand set. It can be used as an intercom, that is, people using the two units can talk to each other, which made it quite useful for tests. The base unit came with a half-wave whip antenna, while the handset came with a quarter-wave whip. As best as could be determined from the service manual, both antennas were connected, without matching networks, to 50 Ω duplexers in identical radio units. The transmitters are rated at 0 to -3 dBm. One operates on 30 channels around 903 MHz and the other operates on 30 channels around 927 MHz. 915 MHz was therefore chosen as the design frequency for the new antennas.

The primary design objective was to find antennas that would be about flush with the cases of the two units. Since the handset is used in a vertical position, it was decided to try an antenna consisting of a wire coming up from the radio box to a rectangular plate in the top of the handset. The radio boxes are electrically closed and so were treated as given end bodies. Their length dimension is 90 mm, which is electrically rather long at 915 MHz (λ_0=328 mm). This allowed a plate thickness and wire size to be found that gives an input impedance of close to 50 Ω. The radio box in the base unit is horizontal, so its vertical dimension is only 16 mm. The box and antenna assembly were designed to be inductive so that only a shunt capacitor is needed to tune them up to 50 Ω.

The numerical exploration was first done by approximating the box and plate with equal-area cylinders, using a version of the body-of-revolution code of [7] modified to remove the requirement for a structure with symmetry about the feed point. Then wire grid models were developed and used in EZNEC-M [9], a software package that uses NEC2S as its analysis engine. The wire grid models are shown in Figure 6. Figures 7-9 show photographs of the two units with their original antennas laid out and the new ones installed. Note the variable tuning capacitor on the base unit.

Before the original antennas were removed, the radios were tested to see at what distance the link failed. This was found to be nearly two blocks, about 1/6 mile. Their signal levels on transmit were also observed on a spectrum analyzer with a commercial 900 MHz monopole on its input. When the new antennas were put on, the handset appeared to give about the same signal strength as the original whip. The base unit gave a little less. This was confirmed by a distance test, on the same path as the originals were tested, in which the fail range was found to be about 1.5 blocks. We attribute this to the greater directivity of the half-wave whip over a short monopole. It was also observed that the handset was less subject to detuning by proximity to a head than the original whip.

6. Conclusions

The chief advantage of this class of shapes is that the antenna is usable near its resonant frequency in the same way as a standard unloaded antenna of much greater length. For many kinds of radio service, a single simple matching network will cover the entire service frequency range. The size reduction will allow the antenna to be hidden in the radio package for many applications. The control of reactance at the design frequency allows impedance-matching losses to be kept low. Network losses are the chief cause of system inefficiency for short dipoles since, like the

antennas in Tables 2-4, they are themselves quite low in loss.

The results reported in this paper represent only a modest beginning for research, development, and application. An interesting question is, where does a thick plate become a thin plate? We know a thin plate can be modeled as a system of wires, for which there is no question that the current goes to zero at their open ends. The assumptions underlying the software available to the author are not valid for thin plates or very acute edges. The results on different shapes are illustrative, but different readers will have their own specific concerns and questions. Here is an opportunity for rigorous testing on various antenna ranges for both efficiency and near-field properties. As the cordless phone example shows, every new application is an opportunity to make a different parameter trade-off study, either numerically or experimentally.

Acknowledgement

The author would like to thank Ron Mason and Dennis Loban for building, installing, and testing the cordless phone antenna set.

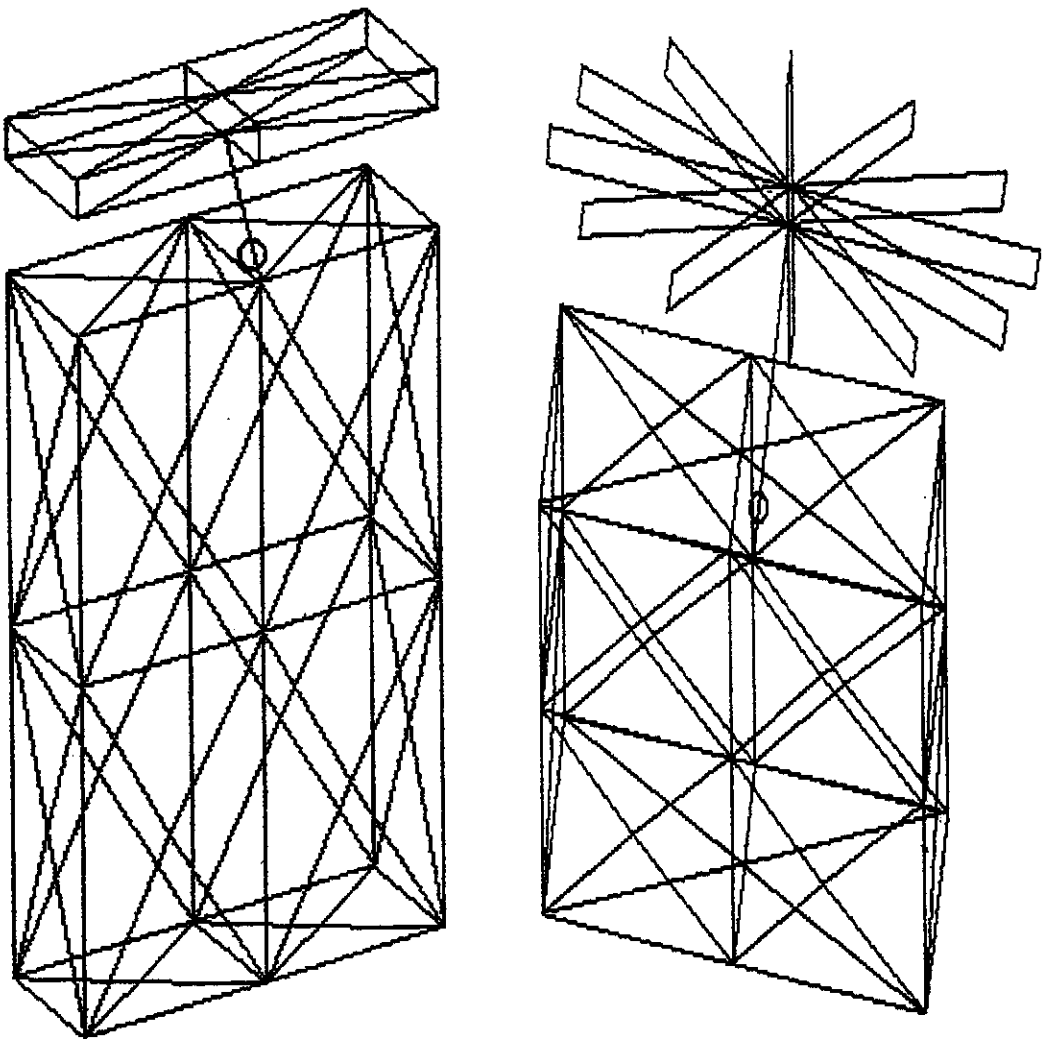

Figure 6. Wire-grid models used in EZNEC-M. The handset is modeled on the left. It is fed from the edge of the radio box because that's where the PC board and track come out. The base unit is modeled on the right. The radio box model is the same in both cases. They look different because of the rotations required to see the antenna models clearly.

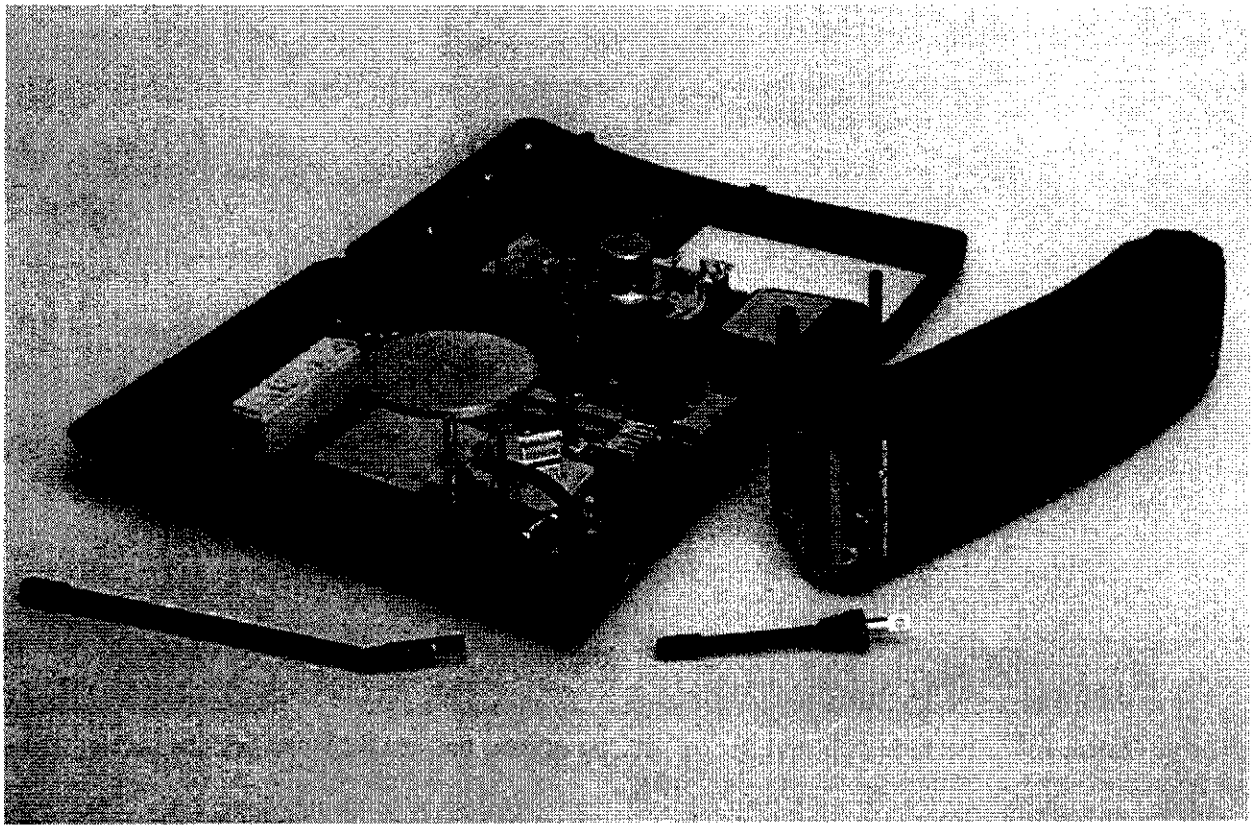

Figure 7. Photo of cordless phone base unit on left, handset on right, and their original stick antennas along the bottom.

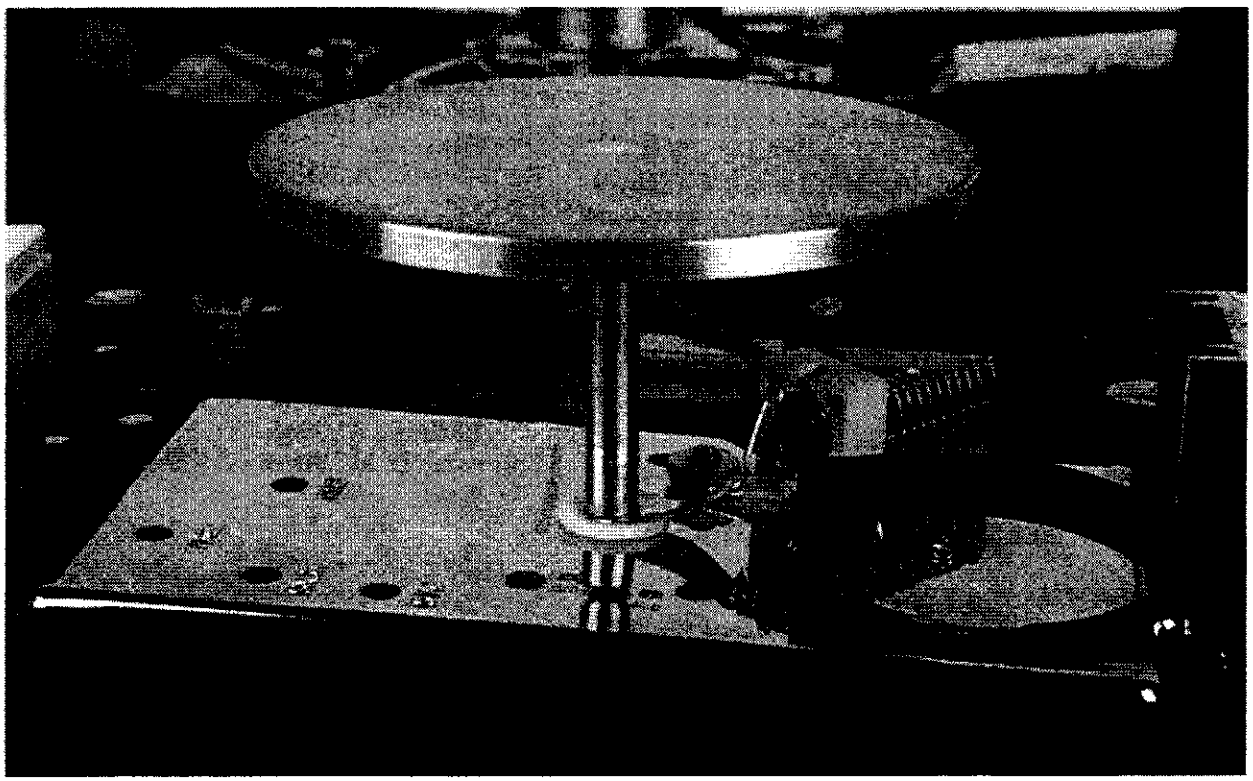

Figure 8. Closeup of base unit radio box, antenna, and tuning capacitor.

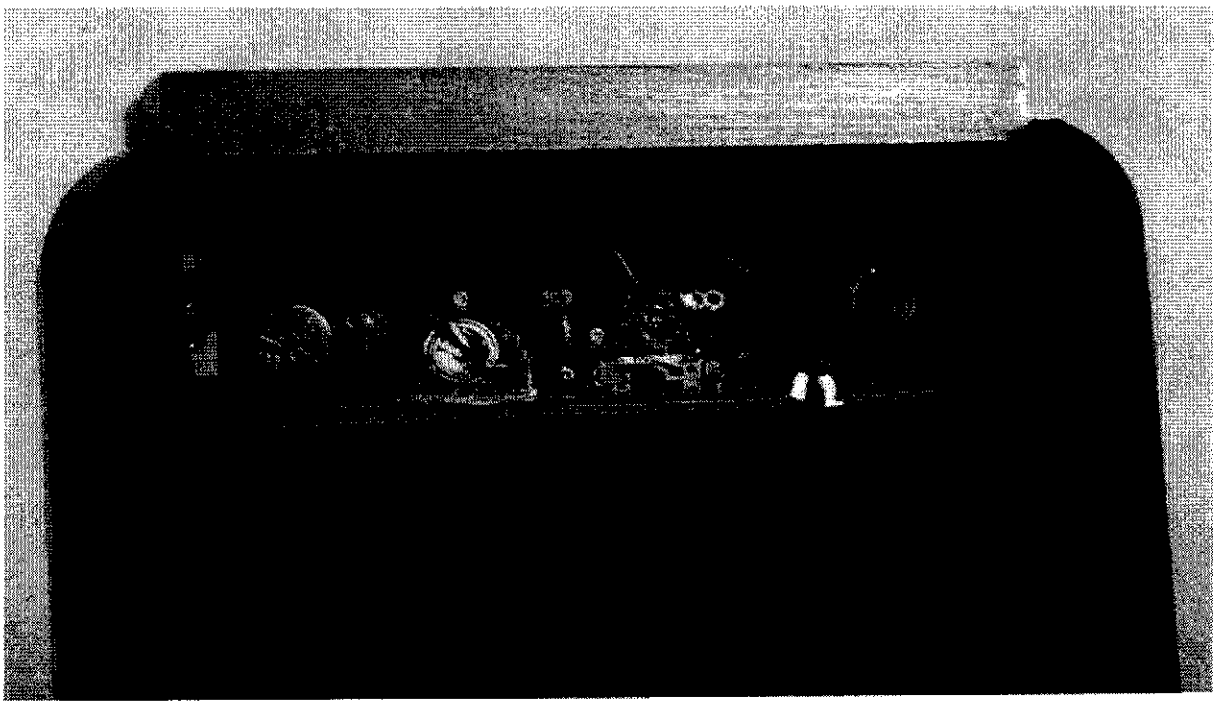

Figure 9. Closeup of handset antenna plate, edge on, with top of radio box and PC board partially visible. The solder joint and the antenna wire are visible in the center of the photo.

Appendix

Standing wave ratio, S, and impedance magnitude, $|Z|$, can be converted into R and $|X|$ as follows. Let Γ be the reflection coefficient. Then, by definition $S=(1+|\Gamma|)/(1-|\Gamma|)$, so $|\Gamma|=(S-1)/(S+1)$ is known. Let $M=|\Gamma|^2$. Then $M=[(R-Z_o)^2+X^2]/[(R+Z_o)^2+X^2]$ which can be solved for R to give $R=(|Z|^2+Z_o^2)(1-M)/[2Z_o(1+M)]$. Then $|X|=(|Z|^2-R^2)^{0.5}$. Foster's Reactance Theorem [10, p213ff] says that $dX/d\omega>0$ for a lossless network. While the antennas discussed here are not lossless, away from resonance they are definitely low-loss one-ports, so one expects the slope of X to be positive. Therefore, if $|X|$ is decreasing, its sign must be negative.

References

[1] McLean, J. S., "A Re-Examination of the Fundamental Limits on the Radiation Q of Electrically Small Antennas", IEEE Trans. Vol. AP-41, pp672-676, May 1996.

[2] Wheeler, H. A., "Small Antennas" in **Antenna Engineering Handbook**, 3rd ed., R. C. Johnson editor, McGraw-Hill, 1993.

[3] Stutzman and Thiele, **Antenna Theory and Design**, pp79-84, Wiley, 1981.

[4] **ARRL Antenna Book**, pp2-37, 16-3, 16-13, G. Hill editor, ARRL, 1991.

[5] Hansen, R. C., "Efficiency and Matching Tradeoffs for Inductively Loaded Short Antennas", IEEE Trans. Vol. COM-23, pp430-435, April 1975.

[6] Fournier and Pomerleau, "Experimental Study of an Inductively Loaded Short Monopole Antenna", IEEE Trans. Vol. VT-27, pp1-6, February 1978.

[7] Miron, D. B., "The Short Fat Dipole; Development in APL of a MoM Solution", J. ACES, vol. 6, no. 2, Winter, 1991.

[8] Mautz, J. R. and R. F. Harrington, "Radiation and Scattering from Bodies of Revolution", Applied Scientific Research, vol. 20, June 1969.

[9] Lewallen, Roy, **EZNEC-M**, w7el@teleport.com, or Roy Lewallen P.E., P.O. Box 6658, Beaverton, OR 7007, U.S.A., 1996.

[10] Pozar, D. M., **Microwave Engineering**, Addison-Wesley, 1990.